Published in final edited form as:

Nat Cell Biol. 2015 May ; 17(5): 639–650. doi:10.1038/ncb3129.

EARP, a multisubunit tethering complex involved in endocytic recycling

Christina Schindler[1,2], **Yu Chen**[1,2], **Jing Pu**[1], **Xiaoli Guo**[1], and **Juan S. Bonifacino**[1,3]

[1]Cell Biology and Metabolism Program, *Eunice Kennedy Shriver* National Institute of Child Health and Human Development, National Institutes of Health, Bethesda, Maryland, 20892, USA

Abstract

Recycling of endocytic receptors to the cell surface involves passage through a series of membrane-bound compartments by mechanisms that are poorly understood. In particular, it is unknown if endocytic recycling requires the function of multisubunit tethering complexes, as is the case for other intracellular trafficking pathways. Herein we describe a tethering complex named Endosome-Associated Recycling Protein (EARP) that is structurally related to the previously described Golgi-Associated Retrograde Protein (GARP) complex. Both complexes share the Ang2, Vps52 and Vps53 subunits, but EARP comprises an uncharacterized protein, Syndetin, in place of the Vps54 subunit of GARP. This change determines differential localization of EARP to recycling endosomes and GARP to the Golgi complex. EARP interacts with the target-SNARE Syntaxin 6 and various cognate SNAREs. Depletion of Syndetin or Syntaxin 6 delays recycling of internalized transferrin to the cell surface. These findings implicate EARP in canonical membrane-fusion events in the process of endocytic recycling.

INTRODUCTION

Plasma membrane proteins are internalized via vesicular carriers that transport cargo to early endosomes. Once in endosomes, the fates of internalized proteins diverge. Some proteins are transported to lysosomes by either staying within the limiting membrane or budding into intraluminal vesicles while early endosomes mature to late endosomes[1]. Other internalized proteins exit endosomes by way of tubular-vesicular carriers that deliver proteins to the *trans*-Golgi network (TGN)[2], to specialized storage organelles such as the insulin-responsive GLUT4 compartment[3] and melanosomes[4], or back to the plasma membrane ("endocytic recycling")[5]. This latter pathway is complex, involving various recycling intermediates and, in polarized cells, sorting to different plasma membrane domains.

[3]Correspondence should be addressed to J.S.B. (bonifacinoj@helix.nih.gov), T: 301-496-6368; F: 301-402-0078.
[2]These authors contributed equally to this work

AUTHOR CONTRIBUTIONS

C.S., Y.C. and J.S.B. conceived the project. C.S. and Y.C. performed most of the experiments. J.P contributed to SNARE pulldowns and X.G. to subcellular fractionation experiments. C.S., Y.C., J.P., X.G. and J.S.B. analyzed the data. J.S.B., C.S. and Y.C. wrote the manuscript.

COMPETING FINANCIAL INTERESTS

The authors declare no competing financial interests.

The ability of proteins to navigate this maze of post-endocytic transport pathways depends on an array of molecular machineries that function at different stages of the endomembrane system. In recent years, substantial progress has been made in the elucidation of the mechanisms that mediate retrograde transport from endosomes to the TGN[6,7]. A key player in these mechanisms is a multisubunit complex named “retromer”, which promotes cargo sorting into membrane tubules that bud from endosomes[8,9,10]. The resulting transport intermediates fuse with the TGN by virtue of a SNARE complex formed by the vesicle-SNARE (or R-SNARE) VAMP4 and the target-SNAREs (or Q-SNAREs) Syntaxin 6 (Stx6), Stx16 and Vti1a[11]. Assembly of these SNAREs is regulated by the TGN-associated, multisubunit tethering complex GARP (for Golgi-Associated Retrograde Protein), which is composed of four subunits named Ang2 (a.k.a. Vps51), Vps52, Vps53 and Vps54[12].

Recycling of internalized proteins from endosomes to the plasma membrane also involves segregation into tubular intermediates[13], but the mechanisms responsible for cargo sorting as well as formation and consumption of the tubules are less well understood[14]. These tubules participate in fast and slow recycling pathways that are characterized by the association with the small GTPases Rab4[15,16] and Rab11[17,18,16], respectively. The slow pathway includes passage through a pericentriolar organelle referred to as the “endocytic recycling compartment” (ERC)[19]. Endocytic recycling is likely a dissociative process involving budding and fusion of membrane-enclosed transport intermediates, as suggested by the implication of several SNARES, including VAMP4[20], Stx6[20,21,22,23], Stx16[24,25] and Vti1a[26,27], as well as VAMP3/cellubrevin[28,29,30,22] and Stx13[31,32,33,34], in this pathway. The exact composition of SNARE complexes and the specific steps in which they function in this pathway, however, remain to be determined. Furthermore, SNARE-mediated fusion generally involves tethering complexes, but to date none have been shown to function in endocytic recycling.

In the course of studies on GARP, we obtained insights into tethering complexes that participate in endocytic recycling. A search for GARP interactors resulted in the identification of a previously uncharacterized protein herein named “Syndetin” that assembles with Ang2, Vps52 and Vps53 – but not Vps54 – to form another complex named “EARP” (for “Endosome-Associated Recycling Protein”). Significantly, EARP associates with Rab4-positive endosomes, while GARP mainly localizes to the TGN. Functional analyses show that EARP and, to a lesser extent, GARP promote recycling of internalized transferrin (Tf) receptor (TfR) to the plasma membrane, most likely through their roles as tethering factors for a set of endosomal SNAREs. These findings highlight the hitherto unknown requirement for multisubunit tethering complexes in the process of endocytic recycling.

RESULTS

Identification of Syndetin as a GARP-subunit interactor

In experiments aimed at identifying proteins that interact with GARP, we performed tandem affinity purification and mass spectrometry using detergent extracts from H4 human neuroglioma cells stably expressing One-STrEP/FLAG (OSF)-tagged human GARP subunits. We set a threshold of 10 unique peptides per protein in the mass spectrometry

results to limit our analyses to the most abundant interactors. Initial experiments using Ang2-OSF as bait yielded 10 proteins above the threshold (Fig. 1a). Four of the five top hits corresponded to the GARP subunits Ang2, Vps52, Vps53 and Vps54, verifying the specificity of the method (Fig. 1a). Surprisingly, the top hit was an uncharacterized protein of 964 amino acids termed CCDC132 (coiled coil domain containing protein 132) (isoform a; NP_060137.2). We renamed this protein "Syndetin" (from the Greek *syndeo*: to connect or tether) because of its structural similarity to other tethering proteins (see below). Likewise, analyses using Vps52-OSF and Vps53-OSF as baits yielded Syndetin and the four GARP subunits as the top five hits (Fig. 1a). Similar analyses using Syndetin-OSF resulted in the co-isolation of Ang2, Vps52, and Vps53, but, remarkably, not Vps54 (Fig. 1a). These observations raised the possibility that Syndetin was a component of a GARP complex variant lacking Vps54. The remaining five proteins that co-isolated with Ang2-OSF did not co-purify with Vps52-OSF, Vps53-OSF or Syndetin-OSF (Fig. 1a), and were thus deemed unlikely to represent specific GARP interactors.

Protein sequence analysis using the HHpred tool[35] showed homology of Syndetin to Vps54 (significance value E=5.5e^{-92}) and, to a lesser extent, Vps53 (E=4.9e^{-05}), as well as the Sec8 (E=1e^{-10}) and Sec15 (E=2e^{-11}) subunits of the exocyst complex, and the Cog2 (E=1.4e^{-10}) and Cog5 (E=1.4e^{-10}) subunits of the COG complex. All of these proteins are subunits of multisubunit tethering complexes that are structured as tandem repeats of an α-helical bundle fold named CATCHR (for Complex Associated with Tethering Containing Helical Rods)[36]. Indeed, secondary structure predictions indicated that Syndetin has α-helical N- and C-terminal regions (corresponding to Domains of Unknown Function DUF2450 and DUF2451, respectively), connected by a less structured middle region (Fig. 1b and Supplementary Fig. 1). Moreover, the Phyre2 protein fold recognition server[37] predicted that both Syndetin and Vps54 are structured as five or six tandemly arranged CATCHR modules (Fig. 1c). Syndetin is thus likely a member of the CATCHR family of tethering proteins and the one that is most closely related to Vps54.

Phylogenetic analyses identified orthologs of both Syndetin (Fig. 1d and Supplementary Fig. 1) and Vps54 in all eukaryotic super-groups (categorized according to ref. [38]), indicating that the two proteins arose from gene duplication in a common eukaryotic ancestor. A few groups, however, seem to have lost expression of Syndetin (*e.g.*, fungi and entamoebida), or both Syndetin and Vps54 (*e.g.*, rhizaria and non-bony fish), over the course of evolution (Fig. 1d). The presence of both Syndetin and Vps54 in such a wide range of eukaryotes suggests that they fulfill critical, yet distinct functions.

Syndetin is a component of a GARP complex variant lacking Vps54

Immunoblot analysis using antibodies to Syndetin, Vps52 and Vps53 showed expression of the three proteins in all mouse tissues examined, with highest levels in different areas of the brain, as well as kidney and testis (Fig. 2a). They were also expressed in human cell lines such as HeLa (Fig. 2a). Subcellular fractionation of HeLa cells revealed that Syndetin, Vps52 and Vps53 were mainly associated with membranes, from which they could be extracted by treatment with 1 M NaCl or 1% Triton X-100 (Fig. 2b). Thus, these proteins behaved as peripheral membrane components. Further analyses of the NaCl-extracted

proteins by sedimentation velocity on linear glycerol gradients (Fig. 2c) and size-exclusion chromatography on Superose 6 (Fig. 2d) showed that Syndetin behaved as a monodisperse species with hydrodynamic properties similar to those of GARP (sedimentation coefficient $S_{20,w}$=9.3 S; Stokes radius *Rh*=91Å; calculated molecular mass M_r=360 ± 20 kDa)[39].

To directly assess the relationship of Syndetin to GARP, we analyzed cell lysates by immunoprecipitation with antibody to Syndetin followed by immunoblotting with antibodies to Ang2, Vps52 and Vps53. We found that Syndetin co-precipitated with Ang2, Vps52 and Vps53 in both HeLa cells (Fig. 2e, left panel) and rat cortical neurons (Fig. 2e, right panel). We could not test if Syndetin assembles with Vps54 using this protocol because of the lack of a suitable antibody to Vps54. To overcome this limitation, we applied the same immunoprecipitation-immunoblotting protocol to HeLa cells transiently expressing Ang2, Vps52, Vps53 and Vps54, all tagged with the V5 epitope[39]. We observed that the antibody to endogenous Syndetin brought down V5-tagged Ang2, Vps52 and Vps53, but not Vps54 (Fig. 2f). Reciprocally, the antibody to the V5 epitope brought down endogenous Syndetin from cells expressing V5-tagged Ang2, Vps52 and Vps53, but not Vps54 (Fig. 2g). Finally, we examined pairwise interactions using the yeast two-hybrid system and found preferential interactions of both Syndetin and Vps54 with Vps53 (Fig. 2h). Taken together, these experiments indicated that Syndetin is a subunit of a complex comprising Ang2, Vps52 and Vps53, but not Vps54. The sum of the predicted molecular masses of Syndetin (111 kDa), Ang2 (86 kDa), Vps52 (82 kDa) and Vps53 (80 kDa) is 359 kDa, similar to the molecular mass calculated from hydrodynamic measurements of the Syndetin-containing complex, consistent with it being a 1:1:1:1 heterotetramer. This complex differs from the previously characterized human GARP[39] in having Syndetin in place of Vps54. For reasons that will become apparent in the following sections, we refer to this complex as “EARP” (for “Endosome-Associated Recycling Protein”).

Syndetin and Vps54 confer distinct intracellular localizations on their corresponding complexes

Next we examined the intracellular localization of Syndetin in comparison to Vps54. Because antibodies to these proteins do not work for immunostaining, we performed confocal immunofluorescence microscopy on cells expressing tagged proteins. Initial experiments were performed with rat hippocampal neurons because of the high expression levels of these proteins in the brain (Fig. 2a), which ensured an abundance of the cognate subunits. We observed that Vps54-EGFP perfectly co-localized with the TGN marker p230 (Fig. 3a). In contrast, Syndetin-EGFP was found in punctate foci scattered throughout the cytoplasm of the soma and dendrites, and did not significantly co-localize with p230 (Fig. 3b) or Vps54-13myc (Fig. 3c). Live-cell imaging of H4 neuroglioma cells co-expressing Vps54-EGFP and Syndetin-mCherry also showed predominant localization of these proteins to the TGN and cytoplasmic puncta, respectively (Fig. 3d and Supplementary Video 1). The lower background in these cells allowed us to observe a population of Vps54-EGFP in cytoplasmic puncta containing Syndetin-mCherry (Fig. 3d and Supplementary Video 1). From these experiments, we concluded that Syndetin localizes to punctate cytoplasmic structures, whereas Vps54 localizes largely to the TGN and, to a lesser extent, to the same punctate structures that contain Syndetin.

We also compared the localizations of tagged Vps54 and Syndetin with those of tagged Ang2 and Vps53, co-expressed in a pairwise manner in rat hippocampal neurons. Interestingly, we observed that in Vps54-EGFP-expressing cells, Vps53-13myc (Fig. 3e) and Ang2-13myc (Supplementary Fig. 2a) co-localized with Vps54-EGFP at the TGN, whereas in Syndetin-EGFP-expressing cells, Vps53-13myc (Fig. 3f) and Ang2-13myc (Supplementary Fig. 2a) co-localized with Syndetin-EGFP on punctate structures. Therefore, Vps54 and Syndetin are the subunits that specify the localization of their corresponding complexes to the TGN and to punctate structures, respectively.

Syndetin localizes to Rab4-containing endosomes involved in transferrin receptor recycling

To identify the punctate structures containing Syndetin, we compared the localization of Syndetin-EGFP to that of various endosomal markers in rat hippocampal neurons (Fig. 4). The best co-localization was observed for Syndetin-EGFP with TagRFP-Rab4A by live-cell, total internal reflection fluorescence (TIRF) microscopy, which enabled low-background visualization of cytoplasmic particles within a ~200-nm evanescent field (Fig. 4a–c and Supplementary Video 2). Because TIRF could under-report perinuclear pools of these proteins, we additionally performed confocal microscopy of live HeLa cells expressing Syndetin-EGFP with TagRFP-Rab4A; under these conditions, we could also observe co-localization of these two proteins on punctate structures distributed throughout the cytoplasm (Supplementary Video 3). Rab4A is associated with an endosomal domain that mediates fast endocytic recycling[15]. We also observed significant, albeit less extensive, co-localization of Syndetin-GFP with TagRFP-Rab11A (Fig. 4a,c), a marker for a different endosomal domain involved in slow endocytic recycling[17,18]. Less co-localization was observed for Syndetin-GFP and TagRFP-Rab5A (Fig. 4a,c and Supplementary Video 4), a marker for early endosomes[40,41].

Endosomal domains containing Rab5 and Rab4 represent consecutive stages in the recycling of endocytic receptors such as the transferrin (Tf) receptor (TfR) back to the cell surface[16]. Consistent with the placement of Syndetin in this pathway, live-cell imaging using HeLa cells showed that Tf-Alexa568 accessed a Syndetin-4xEGFP compartment as early as 3 min after internalization, and its presence in this compartment increased for up to 20 min (Fig. 5 and Supplementary Video 5). From these experiments, we concluded that Syndetin localizes mainly to Rab4-containing endosomes involved in TfR recycling to the cell surface.

Syndetin regulates endocytic recycling of the transferrin receptor

To investigate the function of Syndetin, we performed siRNA-mediated knock down (KD) in HeLa cells and examined the cells for various trafficking phenotypes. Syndetin KD was quite efficient (>90% depletion) and also caused large reductions in the amounts of Vps52 and Vps53 (Fig. 6a), indicating that most of the latter proteins exist as subunits of EARP rather than GARP. Moreover, KD of Ang2, Vps52 or Vps53 depleted not only the primary targets of the siRNAs but also the other proteins, including Syndetin (Fig. 6a). Syndetin KD had no effect on the levels of the autophagy marker LC3-II, in contrast to Ang2, Vps52, Vps53 or Vps54 KD, which greatly increased them (Fig. 6a)[39]. Treatment with the lysosome acidification inhibitor bafilomycin A1 abolished these differences in LC3-II levels

(Supplementary Fig. 4b), suggesting that they were due to impaired lysosomal degradation of LC3-II in GARP-deficient but not EARP-deficient cells. These findings are consistent with the known requirement of GARP for sorting of acid hydrolases to lysosomes[42], and suggest that EARP is not involved in this process. Confocal microscopy showed that Syndetin KD had no effect on retrograde transport of internalized Shiga toxin B subunit (STxB) to the Golgi complex and steady-state localization of TGN46 to the TGN (Supplementary Fig. 2b), in contrast to Ang2 or Vps54 KD, which caused accumulation of these proteins in endosomal intermediates (Supplementary Fig. 2b)[39,42,43,44]. These experiments thus demonstrated that, unlike GARP, the Syndetin-containing complex is not involved in retrograde transport from endosomes to the TGN.

The localization of Syndetin to Rab4A-containing endosomes prompted us to test its requirement for endocytic recycling of the TfR. The initial internalization rate of Tf-Alexa568 after 3 min of uptake was similar in mock-, Syndetin- and Vps54-KD cells, indicating that these proteins are not involved in Tf endocytosis (Supplementary Fig. 3a,b). At later times, however, Syndetin-KD cells, and to a lesser extent Vps54-KD cells, accumulated more intracellular Tf-Alexa568 than mock-treated cells (Supplementary Fig. 3c). To determine if this increased accumulation was due to decreased recycling, mock-, Syndetin- and Vps54-KD HeLa cells were allowed to internalize Tf-Alexa568 for 20 min, after which the cells were chased for different times and intracellular fluorescence was quantified by live-cell imaging. We observed that the intracellular fluorescence was lost more rapidly in mock-treated ($t_{1/2}$=6 min) than in Syndetin-KD cells ($t_{1/2}$=15 min) (Fig. 6b,c). Expression of siRNA-resistant mouse Syndetin, but not Vps53, rescued Tf-Alexa568 recycling (Fig. 6b,c). The retained Tf-Alexa568 in Syndetin-KD cells partly accumulated in a Rab4A-containing compartment as observed by fluorescence microscopy (Fig. 6d). Subcellular fractionation of Syndetin-KD cells also showed partial accumulation of Tf-biotin in a light fraction that co-sedimented with Rab4, although the majority of Tf-biotin was found in a heavier fraction that partly overlapped with Lamp-1 (Supplementary Fig. 4a). This latter fraction might reflect the rerouting of the retained Tf-biotin to lysosomes. These experiments thus demonstrated that Syndetin is required for efficient recycling of the TfR. Vps54 KD also delayed Tf-Alexa568 recycling, albeit to a lesser extent ($t_{1/2}$=11 min) (Fig. 6b,c). This may indicate a recycling role for the small population of Vps54 that co-localizes with Syndetin on endosomes (Fig. 3d).

EARP interacts and co-localizes with endosomal SNAREs

GARP interacts with the Stx6-Stx16-Vti1a-VAMP4 SNARE complex involved in fusion of endosome-derived transport carriers to the TGN[43,45]. Interactions are mainly mediated by binding of the regulatory Habc domain of Stx6 to an N-terminal motif in the Ang2 subunit of GARP[43,45]. Since EARP also comprises Ang2 as one of its subunits, we expected it to interact with a similar set of SNAREs. Indeed, Syndetin-OSF pulldowns from H4 cells resulted in the co-isolation of endogenous Stx6, Stx16, Vti1a and VAMP4, as well as the Stx6-interacting, recycling endosomal SNAREs Stx13[20] and VAMP3[46,11,22] (Fig. 7a). In contrast, Syndetin-OSF did not pull-down two other SNAREs, Stx2 and Stx4, that are involved in exocytosis at the plasma membrane[47,48] (Fig. 7a). Moreover, Stx6, Stx16, Vti1a, VAMP4, Stx13 and VAMP3 exhibited varying degrees of co-localization with Rab4A on

cytoplasmic puncta in HeLa cells (Fig. 7b). Finally, Stx6 KD also delayed recycling of the TfR (Fig. 7c). These findings suggest that EARP acts on Stx6, likely in conjunction with a set of endosomal SNAREs, to promote TfR recycling to the plasma membrane.

DISCUSSION

Our search for interactors of the GARP complex resulted in the unexpected discovery of a structurally related complex, EARP, in which Vps54 is substituted by a previously uncharacterized protein herein named Syndetin. Vps54 and Syndetin are the key subunits that determine distinct localization of GARP to the TGN and EARP to recycling endosomes. Most importantly, while GARP is mainly involved in retrograde transport from endosomes to the TGN[42,43,39,44], EARP is required for recycling of internalized TfR to the cell surface (Fig. 8). A small population of GARP also localizes to recycling endosomes and contributes to TfR recycling. Because multisubunit tethering complexes generally promote SNARE-mediated fusion[36,49], the requirement of EARP (and to a lesser extent GARP) in endocytic recycling supports the notion that this process involves transfer between discontinuous membrane-bound compartments.

The implication of EARP in endocytic recycling poses the question of what SNAREs participate in this process. The Ang2, Vps52 and Vps53 subunits shared by GARP and EARP engage in multiple interactions with components of the Stx6-Stx16-Vti1a-VAMP4 complex[43,39,45], which functions in fusion of endosome-derived intermediates with the TGN[11]. Among these interactions, the strongest and most specific occurs between Ang2 and Stx6[39,45]. Since Ang2 is also a component of EARP, it is logical to find co-isolation of Syndetin with Stx6 in affinity-purification experiments. Moreover, Stx6 partially co-localizes with Rab4A on endosomal structures, and Stx6 KD delays TfR recycling. These observations are consistent with Stx6 being one of the SNAREs that are regulated by EARP in the process of endocytic recycling (Fig. 8). This conclusion is in line with the notion that Stx6 is a promiscuous SNARE[50] that functions not only in endosome-to-TGN transport[11] but also in recycling of integrins to the cell surface[21,22] and the aminopeptidase IRAP to the GLUT4 compartment[23]. The identity of the other SNAREs involved in EARP- and Stx6-dependent endocytic recycling remains to be determined. Stx16[24,25], Vti1a[26,27], Stx13[31,32,33,34] and VAMP3/cellubrevin[28,29,30,22] have all been partly localized to recycling endosomes and/or shown to promote endosomal transport events, and we find that they also co-isolate with Syndetin. Furthermore, a SNARE complex composed of Stx6, Stx13, Vti1a and VAMP4 has been shown to mediate homotypic fusion of early endosomes *in vitro*[20], although it remains to be determined if this complex also plays a role in recycling.

Genome-wide screens identified GARP subunits among various factors required for ricin[51,52] and Pseudomonas exotoxin[51] toxicity. Remarkably, in one of these screens Syndetin was identified as a protein whose depletion *increased* susceptibility to ricin[52]. These findings can now be explained on the basis of the different trafficking events mediated by GARP and EARP. Endosome-to-TGN transport dependent on GARP is an essential step in the itinerary of ricin to its eventual site of action in the cytosol. Recycling from endosomes to the plasma membrane promoted by EARP, on the other hand, is not just

dispensable for retrograde transport of the toxin, but likely diminishes the flow of toxin to the TGN by diverting some of it to the cell surface.

Of the many intercompartmental transport processes that take place in the endomembrane system, transport through recycling endosomes was one for which no multisubunit tethering complexes had been implicated. Our findings now demonstrate a role for EARP, and to some extent GARP, in this process. This discovery should enable future studies on (i) the precise nature of the membrane-bound compartments through which cargos traffic along the endocytic recycling pathway, (ii) the detailed molecular mechanisms of budding and fusion events in this pathway, and (iii) the range of physiological processes (*e.g.*, receptor recycling, integrin-mediated cell adhesion and motility, synaptic plasticity) that are dependent on EARP-dependent transport. Our findings should also contribute to the elucidation of the pathogenesis of progressive cerebello-cerebral atrophy type 2 (PCCA2) caused by mutations in Vps53[53], which in light of our results could result from impairment of both GARP-mediated retrograde transport to the TGN and EARP-mediated recycling to the plasma membrane.

ONLINE METHODS

Antibodies and other reagents

Most antibodies used in this study were described in previous publications[39,42,43,44,54,55]. Mouse monoclonal antibody to Syndetin (FLJ20097) (Clone 2D11, Cat# H00055610-M01) (used at 1:1000 dilution for immunoblotting [IB]) was from Abnova (Taiwan). Mouse monoclonal antibody to the myc epitope (Clone 9B11, Cat# 2276) (used at 1:100 dilution for immunofluorescence microscopy [IF]) and rabbit antibody to LC3 (Clone D11, Cat#3868 (1:4000 for IB) were from Cell Signaling (Danvers, MA). Antibodies to Stx2 (Cat# 110022) (1:1000 for IB), Stx6 (Cat# 110062) (1:1000 for IB), Stx16 (Cat# 110162) (1:1000 for IB), and VAMP4 (Cat# 136002) (1:500 for IB) were from Synaptic Systems (Göttingen, Germany). Antibody to Stx4 (NBP1-87374) (1:1000 for IB) was from Novus Biologicals (Littleton, CO). Antibodies to Rab4 (Cat# 610889) (1:300 for IB) and Vti1a (Cat# 611220) (1:1000 for IB) were from BD Biosciences (San Jose, CA). Antibodies to Rab5 (ab109534) (1:1000 for IB) and Rab11 (ab65200) (1:400 for IB) were from Abcam (Cambridge, MA). Antibody to Lamp-1 (Clone H4A3) (1:250 for IB) was from the Developmental Studies Hybridoma Bank at the University of Iowa (Iowa City, IA). Antibody to human TGN46 (AHP500G) (1:1200 for IF) was from AbD Serotec (Raleigh, NC). Antibody to Giantin (Cat# PRB-114C) (1:3000 for IF) was from Covance (Dedham, MA). Antibodies to p230 (1:3000 for IB and 1:750 for IF) and Stx13 (1:2000 for IB) were gifts from M. Marks (University of Pennsylvania, PA). The antibody to Cog8 (1:1000 for IB) was a gift from M. Krieger (MIT, Cambridge, MA). The antibody to VAMP3/cellubrevin (1:3000 for IB) was a gift from Dr. T. Galli (Institut Jacques Monod, Paris, France). HRP-conjugated secondary antibodies were from GE Healthcare (Piscataway, NJ). Alexa-conjugated secondary antibodies were from Invitrogen (Carlsbad, CA). Alexa488- or Alexa568-conjugated human holo-Tf was from Invitrogen. Biotin-coupled human holo-Tf and Streptavidin-peroxidase polymer were from Sigma-Aldrich (St. Louis, MO).

Recombinant DNA procedures

Plasmids encoding OSF-tagged and V5-tagged Ang2, Vps52, Vps53 and Vps54, as well as the same GARP subunits cloned into the yeast-two-hybrid vectors pGADT7 and pGBKT7, were described before[39,42,43,44]. The plasmid encoding Vps54-GFP[1] was used for subcloning the Vps54 cDNA into pRFP-N1 (Clontech, Mountain View, CA). Full-length human and mouse Syndetin were amplified from whole brain cDNA libraries and cloned in pEGFP-N1 and pmCherry-N1 (Clontech), p4xGFP-N1 (gift from W. Hampe, University of Hamburg, Germany) and pCAG-OSF (provided by W. Sundquist, University of Utah, Salt Lake City, UT). For the generation of stable cell lines, the OSF-tagged versions of Ang2, Vps52, Vps53 and Syndetin were subcloned into pcDNA3.1 (Invitrogen). The 13myc-vector was generated by PCR-amplification of the 13myc epitope from pJB302 (gift of S. Brill, Rutgers University, NJ) and cloning of the epitope into the 3′-end of the multiple cloning site of pCI-neo (Promega, Madison, WI). Full-length Ang2, Vps53 and Vps54 were amplified from the respective V5-constructs and cloned in frame with the 13myc epitope. EGFP- and TagRFP-tagged Rab4A, Rab5A and Rab11A have been described previously[56]. Plasmids encoding Vti1a and Stx13 were gifts from S. Pfeffer (Stanford University) and M. Marks (University of Pennsylvania), respectively.

Tissue extracts, cell culture, transfection and RNAi

Mouse tissue extracts were obtained as described[57]. HeLa and H4 cells were obtained from the ATCC (Manassas, VA) and maintained in DMEM supplemented with 10% fetal bovine serum and antibiotics. DNA transfections were carried out using Lipofectamine 2000 (Invitrogen). H4 cells stably expressing OSF-tagged proteins were obtained by transfection of pcDNA3.1-OSF-tagged Ang2, Vps52, Vps53 or Syndetin and subsequent selection with 1mg/ml G418 (Mediatech, Manassas, VA). Hippocampal and cortical neurons were obtained from Sprague-Dawley rats at embryonic day 18[58]. Neurons were transfected using Lipofectamine 2000 on DIV-3 and analyzed on DIV-7. The siRNAs to Ang2, Vps52, Vps53 and Vps54 have been described before[39,42,43,44]. The siRNAs AGAACAGAUGUACGGUUAA to the coding region of Syndetin, GCAGUUAUGUUGGAAGAUU and CAGCAUAGUUGAAGCAAAU to the coding region of Stx6, and a non-targeting SMARTpool were obtained from Dharmacon (Lafayette, CO). For knock-down (KD) experiments, HeLa cells were transfected twice at 48 h intervals using Oligofectamine (Invitrogen) and analyzed 72 h after the second transfection.

Affinity purification and mass spectrometry

Tandem affinity purification (TAP) was conducted as previously described[59]. Briefly, twenty 15-cm dishes of confluent untransfected H4 cells or H4 cells stably transfected with pcDNA3.1-OSF-tagged Ang2, Vps52, Vps53 or Syndetin were detached with 0.2 mM EDTA in PBS and pelleted by centrifugation. After washing twice with PBS, cells were lysed in 30 ml lysis buffer (50 mM Tris, pH 7.4, 150 mM NaCl, 1 mM EDTA, 0.5% NP-40, 10% glycerol) supplemented with protease inhibitors (Sigma-Aldrich). Clarified supernatants were obtained by two consecutive centrifugations at 13,000 x *g* at 4°C and incubated with 1 ml StrepTactin beads (IBA, Olivette, MO) for 2 h with rotation at 4°C. Beads were washed five times with 50 ml lysis buffer each time. For elution, beads were

incubated for 5 min on ice with 4 ml elution buffer (lysis buffer supplemented with 1/10 volume 10X Biotin Elution Buffer [IBA]). Eluates from four consecutive elutions were pooled and passed through an empty polyprep column (BioRad, Hecules, CA) to ensure complete removal of beads. Eluates were added to 500 µl bead volume EZ view red anti-FLAG beads (Sigma-Aldrich) and incubated for 2 h with rotation at 4°C. Beads were washed five times with 50 ml lysis buffer each time. For elution, beads were incubated for 5 min on ice in 500 µl elution buffer (lysis buffer supplemented with 200 µg/ml 3xFLAG peptide). Eluates from four consecutive elutions were pooled and residual beads removed as described above. Proteins were precipitated using trichloroacetic acid and air-dried pellets were analyzed by LC/MS at the Taplin mass spectrometry facility (Harvard Medical School, Cambridge, MA).

Cell fractionation

HeLa cells from one confluent 10-cm dish were detached by incubation with 0.2 mM EDTA in PBS and pelleted for 3 min at 1000 rpm in a refrigerated tabletop centrifuge. The pellet was washed twice with PBS. Cells were resuspended in 500 µl sucrose buffer (20 mM HEPES, pH 7.4, 250 mM sucrose supplemented with protease inhibitors [Sigma-Aldrich]) and incubated for 10 min on ice. Cells were disrupted by repeated passage through a 25-gauge needle. Nuclei and unbroken cells were removed by centrifugation (2 min, 1,000 x *g*, 4°C). Lysates were further clarified by centrifugation in a tabletop centrifuge (10 min, 13,000 x *g*, 4°C). The clarified lysate was diluted 1:1 with sucrose buffer and divided into four samples (S13). One sample was supplemented with 1/4 volume gel-loading buffer 1 (4X LDS sample buffer [Invitrogen] supplemented with 80 mg DTT per ml). Membranes in the remaining samples were pelleted using a TLA-45 rotor (45 min, 91,000 x *g*, 4°C) (Beckman, Indianapolis, IN). The supernatant from one sample was supplemented with 1/4 volume gel-loading buffer 1 (S100, sucrose). The corresponding pellet was resuspended in an equal volume of gel loading buffer 2 (1/2 volume 4X LDS sample buffer and 1/2 volume 50 mM Tris, 1% SDS supplemented with 80 mg DTT per ml) (P100, sucrose). The supernatant of the remaining two samples was discarded and the pellets were resuspended in either 250 µl high-salt buffer (50 mM Tris, pH 7.4, 1 M NaCl, 1 mM EDTA supplemented with 10% glycerol and protease inhibitors) or 250 µl detergent buffer (50 mM Tris, pH 7.4, 150 mM NaCl, 1% Triton X-100, 1 mM EDTA supplemented with 10% glycerol and protease inhibitors). After 30 min on ice, insoluble material was separated by a second spin at 91,000 x *g*. The salt-extracted membrane fraction (S100, 1 M NaCl) or detergent-extracted membrane fraction (S100, 1% Triton X-100) were supplemented with 1/4 volume gel-loading buffer 1. The corresponding pellets were resuspended in equal volumes of gel-loading buffer 2 to generate samples P100 (1 M NaCl) and P100 (1% Triton X-100). Samples were incubated for 5 min at 95°C and 50 µl of each sample were resolved on 4–12% SDS-PAGE gels (Invitrogen) and analyzed by immunoblotting.

Sedimentation velocity ultracentrifugation

Salt-extracted membrane fractions (S100, 1M NaCl) were prepared as above using HeLa cells from one confluent 10-cm dish as starting material. Five hundred µl of S100 fraction were diluted 1:1 with high-salt buffer to a final glycerol concentration of 5%. A 5–20% glycerol step gradient was prepared by overlaying 400 µl of a 45% sucrose cushion with

high-salt buffer supplemented with 20%, 19.5%, 18%, 16.5%, 15%, 13.5%, 11%, 9.5%, 8%, 6.5% or 5% glycerol (1 ml per step, 11 steps total). Gradients were overlayed with 1 ml of salt-extracted membrane fraction and centrifuged at 169,000 x *g* for 16 h at 4°C in a SW41 rotor (Beckman). Twelve fractions of 1 ml each were collected from the top and precipitated by the addition of 1/10 volume of 6.1 M trichloroacetic acid. Preicipitates were recovered by a 30 min spin at 13,000 rpm in a refrigerated tabletop centrifuge and each pellet was washed with 1 ml ice-cold acetone. Pellets were air-dried and resuspended in 60 µl gel-loading buffer 2. Samples were incubated for 5 min at 95°C and 20 µl of each fraction was resolved by SDS-PAGE and immunoblotting. Sedimentation coefficients ($s_{20,w}$) were estimated as previously described[39].

Gel filtration

One ml of salt-extracted membrane fraction was prepared as above using two confluent 10-cm dishes of HeLa cells as starting material. Proteins were separated on a Superose 6 10/300 GL column (GE Bioscience) equilibrated in high-salt buffer supplemented with 10% glycerol. Forty-eight fractions of 500 µl each were obtained and precipitated using trichloroacetic acid as described above. Air-dried pellets were resuspended in 60 µl gel-loading buffer, incubated for 5 min at 95°C and 20 µl of each second fraction were analyzed by SDS-PAGE gels and immunoblotting. Stokes radii (in Å) were determined as previously described[39]. The molecular mass of EARP was calculated assuming a partial specific volume of 0.72–0.75 cm^3/g.

Co-immunoisolation and StrepTactin pulldown

HeLa cells corresponding to one well of a confluent six-well plate were used per sample. Cells were washed in PBS and lysed in 500 µl lysis buffer for 10 min on ice. Fifty µl of clarified supernatant were supplemented with 1/4 volume of gel-loading buffer and set aside as loading control. Four-hundred µl of the remaining supernatant was supplemented with 30 µl Protein A or Protein G beads (GE Healthcare) and antibody, or 30 µl StrepTactin beads. Samples were incubated for 2 h with rotation at 4°C. Beads were washed three times with 1 ml lysis buffer each and resuspended in 40 µl gel-loading buffer. Samples were incubated for 5 min at 95°C and analyzed by SDS-PAGE on 4–12% SDS gradient gels and immunoblotting.

Yeast two-hybrid assays

Yeast strain AH109 was co-transformed with plasmids using standard methods. Three days after transformation, colonies were picked and overnight liquid culture was set up in SD medium lacking leucine and tryptophan (Clontech). On the following day, cultures were diluted to OD_{600} 0.1 and 5 µl of each culture was spotted onto SD agar plates lacking leucine and tryptophan (+His) or SD agar plates lacking leucine, tryptophan and histidine (-His) supplemented with 0.2 mM 3-amino-1,2,4-triazole (3-AT, MP Bio, Santa Ana, CA). Cell growth was analyzed three days after plating.

Transferrin uptake and chase

Tf uptake and chase in HeLa cells was performed using a modification of a previously described protocol[60]. For uptake of Alexa568-conjugated Tf (Invitrogen), mock- or siRNA-treated cells were placed in uptake medium (MEM, 1% ovalbumin, 25 mM HEPES) supplemented with 40 μg/ml Alexa568-conjugated Tf for 20 min. After washing three times with pre-warmed MEM, cells were chased in chase medium (MEM, 25 mM HEPES, 100 μg/ml human holo-Tf) pre-warmed to 37°C. Live-cell imaging was set to start at 10 min after the beginning of the chase. For uptake of biotin-conjugated Tf, cells were incubated in uptake medium supplemented with 40 μg/ml Tf-biotin for 30 min. After washing twice with citrate buffer (pH 4.6) to remove surface-bound Tf, cells were incubated in chase medium for 30 min before harvesting for subcellular fractionation. Tf-biotin was detected using Streptavidin-peroxidase polymer as per the manufacturer's instructions.

Fluorescence microscopy

Immunofluorescence microscopy was performed as previously described[61,62] on a Zeiss LSM710 microscope (Carl Zeiss, Thornwood, NY). Live-cell imaging was conducted with a NIKON Eclipse Ti Microscope System equipped with an environmental chamber (temperature controlled at 37°C and CO_2 at 5%), high-speed EM charge-coupled device cameras (iXon DU897 from Andor and Evolve 512 from Photometrics), and NIS-Elements Ar Microscope Imaging Software. TIRF Images were acquired with an Apo TIRF 100X objective (N.A. 1.49) and iXon DU897. Spinning-disk confocal z-stacks were taken with a Plan Apo VC 60x H objective (N.A. 1.40) and Evolve 512. Dual-color imaging was achieved by fast switching excitation lasers so that images from green and red channels were aligned automatically.

FACS analysis

Flow cytometry was performed to quantify Tf uptake in the experiment shown in Fig. S3c. HeLa cells transfected with Mock, Vps54 or Syndetin siRNAs were incubated with 40 μg/ml Tf-Alexa647 at 37°C for different times, and washed twice with ice-cold citrate buffer (pH 4.6) and three times with PBS to remove surface-bound Tf. After detaching cells from the plates by incubation with 2 mM EDTA on ice for 1 h, cells were resuspended in ice-cold PBS and kept on ice until analysis by FACS. Suspended cells were analyzed using a FACSCALIBUR (BD Biosciences) equipped with 635-nm red-diode laser and standard filters to detect Alexa647 emission. CellQuest Acquisition and Analysis software was used to quantify at least 1×10^5 cells from each group in each independent experiment.

Statistical analysis

All numerical results are reported as the mean ± SEM and represent data from a minimum of three independent experiments. No statistical method was used to predetermine sample size. The experiments were not randomized, and the investigators were not blinded to allocation during experiments and outcome assessment. GraphPad InStat software (GraphPad, LaJolla, CA) was used for analysis of statistical significance. Unless otherwise indicated, two-tailed Student's *t* test for unpaired data was used to evaluate single comparisons between different experimental groups. Normal distribution of the data sets in comparisons passed D'Agostino

& Pearson omnibus normality test. Differences were considered statistically significant for a value of $P < 0.05$. Figure 4: F test indicates Rab4A group has significantly smaller variance compared with Rab11A group. Figure 6: mock, 301 cells; Vps54 KD, 297 cells; Syndetin KD, 250 cells; Syndetin KD+Vps53, 73 cells; Syndetin KD+mSyndetin, 61 cells; quantified in 3 independent experiments. Figure 7: mock, 162 cells; Stx6 KD, 143 cells; quantified in 3 independent experiments. Figure S3: mock, 171 cells; Vps54 KD, 167 cells; Syndetin KD, 142 cells; quantified in 3 independent experiments. Immunofluorescence and live-cell imaging results shown in Figures 3, 4, 5, 6, 7, S2 and S3 are representative of at least 3 independent experiments. Results in Figures 2d, 2e, 2f, 2g, 2h, 6a and 7a are representative of at least 3 independent experiments. Results in Figures 2b, 2c, 6e and S4 are representative of 2 independent experiments. The experiment in Figure 2a was done once.

Accession number

The secondary accession for the protein sequence of Syndetin (CCDC132 isoform a) is NP_060137.2 (NCBI Protein database).

Supplementary Material

Refer to Web version on PubMed Central for supplementary material.

Acknowledgments

We thank X. Zhu and N. Tsai for expert technical assistance, J. Presley for helpful discussions, and R. Mattera and D. Gershlick for critical review of the manuscript. This work was funded by the Intramural Program of NICHD, NIH (ZIA HD001607).

References

1. Henne WM, Buchkovich NJ, Emr SD. The ESCRT pathway. Dev Cell. 2011; 21:77–91. [PubMed: 21763610]
2. Bonifacino JS, Rojas R. Retrograde transport from endosomes to the trans-Golgi network. Nat Rev Mol Cell Biol. 2006; 7:568–579. [PubMed: 16936697]
3. Leto D, Saltiel AR. Regulation of glucose transport by insulin: traffic control of GLUT4. Nat Rev Mol Cell Biol. 2012; 13:383–396. [PubMed: 22617471]
4. Raposo G, Marks MS. Melanosomes--dark organelles enlighten endosomal membrane transport. Nat Rev Mol Cell Biol. 2007; 8:786–797. [PubMed: 17878918]
5. Maxfield FR, McGraw TE. Endocytic recycling. Nat Rev Mol Cell Biol. 2004; 5:121–132. [PubMed: 15040445]
6. Johannes L, Popoff V. Tracing the retrograde route in protein trafficking. Cell. 2008; 135:1175–1187. [PubMed: 19109890]
7. Cullen PJ, Korswagen HC. Sorting nexins provide diversity for retromer-dependent trafficking events. Nat Cell Biol. 2012; 14:29–37. [PubMed: 22193161]
8. Seaman MN, McCaffery JM, Emr SD. A membrane coat complex essential for endosome-to-Golgi retrograde transport in yeast. J Cell Biol. 1998; 142:665–681. [PubMed: 9700157]
9. Seaman MN. Cargo-selective endosomal sorting for retrieval to the Golgi requires retromer. J Cell Biol. 2004; 165:111–122. [PubMed: 15078902]
10. Arighi CN, Hartnell LM, Aguilar RC, Haft CR, Bonifacino JS. Role of the mammalian retromer in sorting of the cation-independent mannose 6-phosphate receptor. J Cell Biol. 2004; 165:123–133. [PubMed: 15078903]

11. Mallard F, et al. Early/recycling endosomes-to-TGN transport involves two SNARE complexes and a Rab6 isoform. J Cell Biol. 2002; 156:653–664. [PubMed: 11839770]
12. Bonifacino JS, Hierro A. Transport according to GARP: receiving retrograde cargo at the trans-Golgi network. Trends Cell Biol. 2011; 21:159–167. [PubMed: 21183348]
13. Geuze HJ, Slot JW, Strous GJ, Lodish HF, Schwartz AL. Intracellular site of asialoglycoprotein receptor-ligand uncoupling: double-label immunoelectron microscopy during receptor-mediated endocytosis. Cell. 1983; 32:277–287. [PubMed: 6130851]
14. Grant BD, Donaldson JG. Pathways and mechanisms of endocytic recycling. Nat Rev Mol Cell Biol. 2009; 10:597–608. [PubMed: 19696797]
15. van der Sluijs P, et al. The small GTP-binding protein rab4 controls an early sorting event on the endocytic pathway. Cell. 1992; 70:729–740. [PubMed: 1516131]
16. Sonnichsen B, De Renzis S, Nielsen E, Rietdorf J, Zerial M. Distinct membrane domains on endosomes in the recycling pathway visualized by multicolor imaging of Rab4, Rab5, and Rab11. J Cell Biol. 2000; 149:901–914. [PubMed: 10811830]
17. Ullrich O, Reinsch S, Urbe S, Zerial M, Parton RG. Rab11 regulates recycling through the pericentriolar recycling endosome. J Cell Biol. 1996; 135:913–924. [PubMed: 8922376]
18. Ren M, et al. Hydrolysis of GTP on rab11 is required for the direct delivery of transferrin from the pericentriolar recycling compartment to the cell surface but not from sorting endosomes. Proc Natl Acad Sci U S A. 1998; 95:6187–6192. [PubMed: 9600939]
19. Yamashiro DJ, Tycko B, Fluss SR, Maxfield FR. Segregation of transferrin to a mildly acidic (pH 6.5) para-Golgi compartment in the recycling pathway. Cell. 1984; 37:789–800. [PubMed: 6204769]
20. Brandhorst D, et al. Homotypic fusion of early endosomes: SNAREs do not determine fusion specificity. Proc Natl Acad Sci U S A. 2006; 103:2701–2706. [PubMed: 16469845]
21. Tiwari A, et al. Endothelial cell migration on fibronectin is regulated by syntaxin 6-mediated alpha5beta1 integrin recycling. J Biol Chem. 2011; 286:36749–36761. [PubMed: 21880737]
22. Riggs KA, et al. Regulation of integrin endocytic recycling and chemotactic cell migration by syntaxin 6 and VAMP3 interaction. J Cell Sci. 2012; 125:3827–3839. [PubMed: 22573826]
23. Watson RT, Hou JC, Pessin JE. Recycling of IRAP from the plasma membrane back to the insulin-responsive compartment requires the Q-SNARE syntaxin 6 but not the GGA clathrin adaptors. J Cell Sci. 2008; 121:1243–1251. [PubMed: 18388312]
24. Proctor KM, Miller SC, Bryant NJ, Gould GW. Syntaxin 16 controls the intracellular sequestration of GLUT4 in 3T3-L1 adipocytes. Biochem Biophys Res Commun. 2006; 347:433–438. [PubMed: 16828707]
25. Gee HY, Tang BL, Kim KH, Lee MG. Syntaxin 16 binds to cystic fibrosis transmembrane conductance regulator and regulates its membrane trafficking in epithelial cells. J Biol Chem. 2010; 285:35519–35527. [PubMed: 20826815]
26. Bose A, et al. The v-SNARE Vti1a regulates insulin-stimulated glucose transport and Acrp30 secretion in 3T3-L1 adipocytes. J Biol Chem. 2005; 280:36946–36951. [PubMed: 16131485]
27. Kreykenbohm V, Wenzel D, Antonin W, Atlachkine V, von Mollard GF. The SNAREs vti1a and vti1b have distinct localization and SNARE complex partners. Eur J Cell Biol. 2002; 81:273–280. [PubMed: 12067063]
28. McMahon HT, et al. Cellubrevin is a ubiquitous tetanus-toxin substrate homologous to a putative synaptic vesicle fusion protein. Nature. 1993; 364:346–349. [PubMed: 8332193]
29. Galli T, et al. Tetanus toxin-mediated cleavage of cellubrevin impairs exocytosis of transferrin receptor-containing vesicles in CHO cells. J Cell Biol. 1994; 125:1015–1024. [PubMed: 8195285]
30. Daro E, van der Sluijs P, Galli T, Mellman I. Rab4 and cellubrevin define different early endosome populations on the pathway of transferrin receptor recycling. Proc Natl Acad Sci U S A. 1996; 93:9559–9564. [PubMed: 8790369]
31. Prekeris R, Klumperman J, Chen YA, Scheller RH. Syntaxin 13 mediates cycling of plasma membrane proteins via tubulovesicular recycling endosomes. J Cell Biol. 1998; 143:957–971. [PubMed: 9817754]
32. Trischler M, Stoorvogel W, Ullrich O. Biochemical analysis of distinct Rab5- and Rab11-positive endosomes along the transferrin pathway. J Cell Sci. 1999; 112:4773–4783. [PubMed: 10574724]

33. Lee SH, Valtschanoff JG, Kharazia VN, Weinberg R, Sheng M. Biochemical and morphological characterization of an intracellular membrane compartment containing AMPA receptors. Neuropharmacology. 2001; 41:680–692. [PubMed: 11640922]
34. Hoogenraad CC, et al. Neuron specific Rab4 effector GRASP-1 coordinates membrane specialization and maturation of recycling endosomes. PLoS Biol. 2010; 8:e1000283. [PubMed: 20098723]
35. Soding J, Biegert A, Lupas AN. The HHpred interactive server for protein homology detection and structure prediction. Nucleic Acids Res. 2005; 33:W244–8. [PubMed: 15980461]
36. Yu IM, Hughson FM. Tethering Factors as Organizers of Intracellular Vesicular Traffic. Annu Rev Cell Dev Biol. 2010; 26:137–156. [PubMed: 19575650]
37. Kelley LA, Sternberg MJ. Protein structure prediction on the Web: a case study using the Phyre server. Nat Protoc. 2009; 4:363–371. [PubMed: 19247286]
38. Walker G, Dorrell RG, Schlacht A, Dacks JB. Eukaryotic systematics: a user's guide for cell biologists and parasitologists. Parasitology. 2011; 138:1638–1663. [PubMed: 21320384]
39. Perez-Victoria FJ, et al. Ang2/Fat-free Is a Conserved Subunit of the Golgi-associated Retrograde Protein (GARP) Complex. Mol Biol Cell. 2010; 21:3386–3395. [PubMed: 20685960]
40. Gorvel JP, Chavrier P, Zerial M, Gruenberg J. rab5 controls early endosome fusion in vitro. Cell. 1991; 64:915–925. [PubMed: 1900457]
41. Bucci C, et al. The small GTPase rab5 functions as a regulatory factor in the early endocytic pathway. Cell. 1992; 70:715–728. [PubMed: 1516130]
42. Perez-Victoria FJ, Mardones GA, Bonifacino JS. Requirement of the human GARP complex for mannose 6-phosphate-receptor-dependent sorting of cathepsin D to lysosomes. Mol Biol Cell. 2008; 19:2350–2362. [PubMed: 18367545]
43. Perez-Victoria FJ, Bonifacino JS. Dual roles of the mammalian GARP complex in tethering and SNARE complex assembly at the trans-golgi network. Mol Cell Biol. 2009; 29:5251–5263. [PubMed: 19620288]
44. Perez-Victoria FJ, et al. Structural basis for the wobbler mouse neurodegenerative disorder caused by mutation in the Vps54 subunit of the GARP complex. Proc Natl Acad Sci U S A. 2010; 107:12860–12865. [PubMed: 20615984]
45. Abascal-Palacios G, Schindler C, Rojas AL, Bonifacino JS, Hierro A. Structural basis for the interaction of the Golgi-Associated Retrograde Protein Complex with the t-SNARE Syntaxin 6. Structure. 2013; 21:1698–1706. [PubMed: 23932592]
46. Bock JB, Klumperman J, Davanger S, Scheller RH. Syntaxin 6 functions in trans-Golgi network vesicle trafficking. Mol Biol Cell. 1997; 8:1261–1271. [PubMed: 9243506]
47. Hutt DM, Baltz JM, Ngsee JK. Synaptotagmin VI and VIII and syntaxin 2 are essential for the mouse sperm acrosome reaction. J Biol Chem. 2005; 280:20197–20203. [PubMed: 15774481]
48. Kennedy MJ, Davison IG, Robinson CG, Ehlers MD. Syntaxin-4 defines a domain for activity-dependent exocytosis in dendritic spines. Cell. 2010; 141:524–535. [PubMed: 20434989]
49. Hong W, Lev S. Tethering the assembly of SNARE complexes. Trends Cell Biol. 2014; 24:35–43. [PubMed: 24119662]
50. Wendler F, Tooze S. Syntaxin 6: the promiscuous behaviour of a SNARE protein. Traffic. 2001; 2:606–611. [PubMed: 11555414]
51. Moreau D, et al. Genome-wide RNAi screens identify genes required for Ricin and PE intoxications. Dev Cell. 2011; 21:231–244. [PubMed: 21782526]
52. Bassik MC, et al. A systematic mammalian genetic interaction map reveals pathways underlying ricin susceptibility. Cell. 2013; 152:909–922. [PubMed: 23394947]
53. Feinstein M, et al. VPS53 mutations cause progressive cerebello-cerebral atrophy type 2 (PCCA2). J Med Genet. 2014; 51:303–308. [PubMed: 24577744]
54. Farias GG, et al. Signal-mediated, AP-1/clathrin-dependent sorting of transmembrane receptors to the somatodendritic domain of hippocampal neurons. Neuron. 2012; 75:810–823. [PubMed: 22958822]

55. Prabhu Y, et al. Adaptor protein 2-mediated endocytosis of the beta-secretase BACE1 is dispensable for amyloid precursor protein processing. Mol Biol Cell. 2012; 23:2339–2351. [PubMed: 22553349]

56. Chen Y, et al. Rab10 and myosin-Va mediate insulin-stimulated GLUT4 storage vesicle translocation in adipocytes. J Cell Biol. 2012; 198:545–560. [PubMed: 22908308]

57. Li WP, Liu P, Pilcher BK, Anderson RG. Cell-specific targeting of caveolin-1 to caveolae, secretory vesicles, cytoplasm or mitochondria. J Cell Sci. 2001; 114:1397–1408. [PubMed: 11257005]

58. Kaech S, Banker G. Culturing hippocampal neurons. Nat Protoc. 2006; 1:2406–2415. [PubMed: 17406484]

59. Gloeckner CJ, Boldt K, Ueffing M. Strep/FLAG tandem affinity purification (SF-TAP) to study protein interactions. Curr Protoc Protein Sci. 2009; Chapter 19(Unit19.20)

60. Ghosh RN, Gelman DL, Maxfield FR. Quantification of low density lipoprotein and transferrin endocytic sorting HEp2 cells using confocal microscopy. J Cell Sci. 1994; 107:2177–2189. [PubMed: 7983176]

61. Burgos PV, et al. Sorting of the Alzheimer's disease amyloid precursor protein mediated by the AP-4 complex. Dev Cell. 2010; 18:425–436. [PubMed: 20230749]

62. Rojas R, et al. Regulation of retromer recruitment to endosomes by sequential action of Rab5 and Rab7. J Cell Biol. 2008; 183:513–526. [PubMed: 18981234]

a

Protein	Ang2	Vps52	Vps53	Syndetin
Syndetin	51	37	37	33
Ang2	44	27	26	21
Vps53	41	30	60	26
Vps52	40	43	32	24
Vps54	27	21	21	0
SNAP29	21	0	0	0
TfR	19	0	0	0
KifC3	19	0	0	0
Lmnb1	17	0	0	0
Alfm1	10	0	0	0

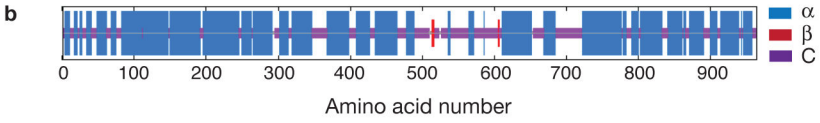

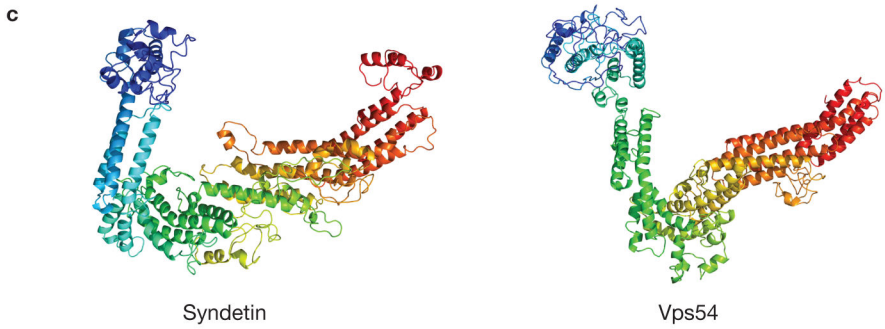

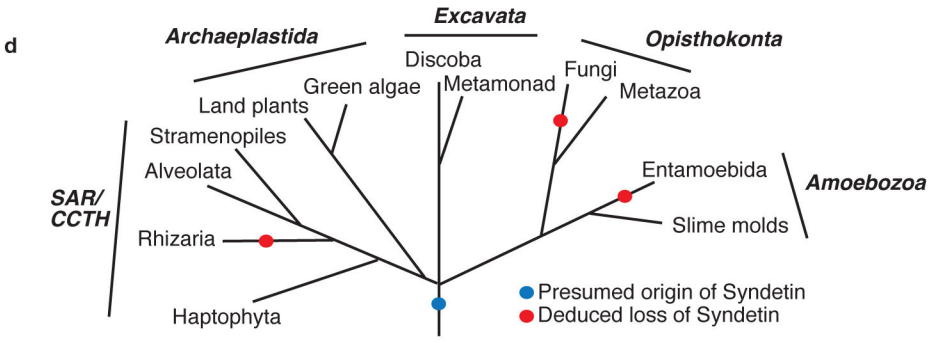

Figure 1.

Identification of Syndetin as a GARP subunit interactor. (**a**) Table listing the most abundant proteins in order of unique peptide number identified by tandem affinity purification and mass spectrometry from Ang2-OSF-expressing H4 cells, and their presence in similar isolates from Vps52-, Vps53- and Syndetin-OSF-expressing cells. (**b**) Consensus secondary structure prediction for human Syndetin using the NPS@ server[63]. Regions predicted to be αhelix, β-sheet and random coil (C) are indicated. (**c**) Predicted tertiary structures of Syndetin and Vps54 according to the Phyre2 server[37]. Individual CATCHR modules are identified by different colors. (**d**) Deduced evolutionary history of Syndetin according to Walker et al.[38].

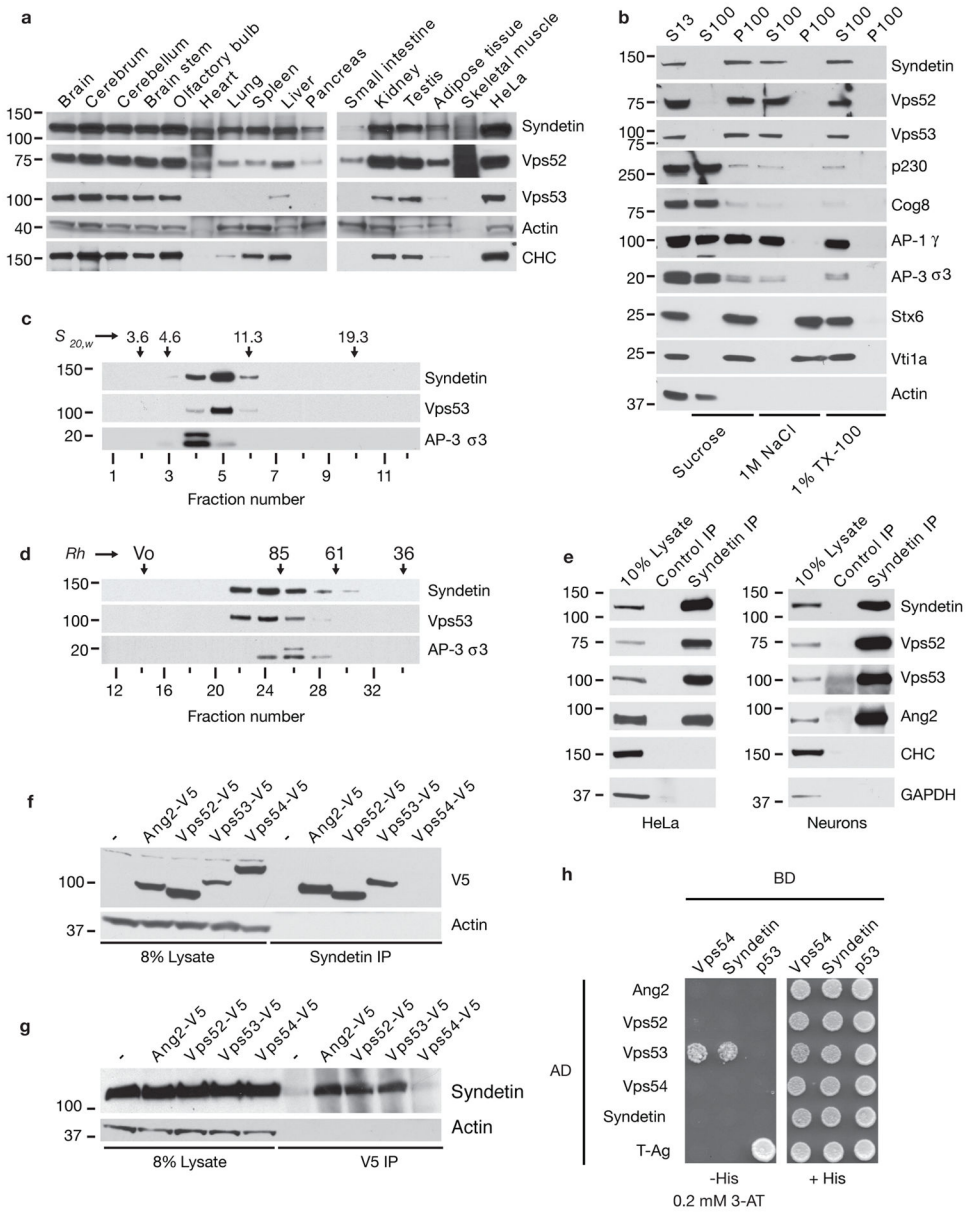

Figure 2.

Biochemical characterization of Syndetin. (**a**) Immunoblot analysis of Syndetin, Vps52, Vps53, actin and clathrin heavy chain (CHC) in different mouse tissues and HeLa cells resolved by SDS-PAGE. (**b**) HeLa cell lysates were fractionated into 13,000 x *g* supernatant (S13), 100,000 x *g* supernatant (S100) and 100,000 x *g* pellet (P100) fractions; P100 was extracted with 1M NaCl or 1% Triton X-100 and further separated into S100 and P100 fractions. (**c,d**) The supernatant from the 1 M NaCl extraction was analyzed by sedimentation velocity on linear 5–20% glycerol gradients (**c**) or size-exclusion chromatography on Superose 6 (**d**). The positions of standard proteins on the gradients (sedimentation coefficient $S_{20,w}$ values in Svedberg units) or the column (Stokes radii *Rh* in Ångstroms) are indicated. Vo: void volume. In **b–d**, fractions were analyzed by SDS-PAGE

and immunoblotting for the indicated proteins. (**e**) Detergent-extracts of HeLa cells (left panel) or rat cortical neurons (right panel) were subjected to immunoprecipitation with antibody to Syndetin followed by SDS-PAGE and immunoblotting with antibodies to the indicated proteins. (**f**,**g**) HeLa cells expressing V5-tagged versions of Ang2, Vps52, Vps53 and Vps54 were extracted in lysis buffer and subjected to immunoprecipitation with antibodies to Syndetin (**f**) or the V5 epitope (**g**), followed by SDS-PAGE and immunoblotting with antibodies to the V5 epitope (**f**) or Syndetin (**g**). In **a**–**g**, molecular mass markers (in kDa) are indicated at left. (**h**) Yeast two-hybrid interaction of Syndetin and Vps54 with Vps53. Growth in the absence of histidine (-His) and presence of 0.2 mM 3-amino-1,2,4-triazole (3-AT) is indicative of interactions. T-Ag, T antigen; AD, activation domain; BD, binding domain. Uncropped images of the blots are shown in Supplementary Fig. 5a and b.

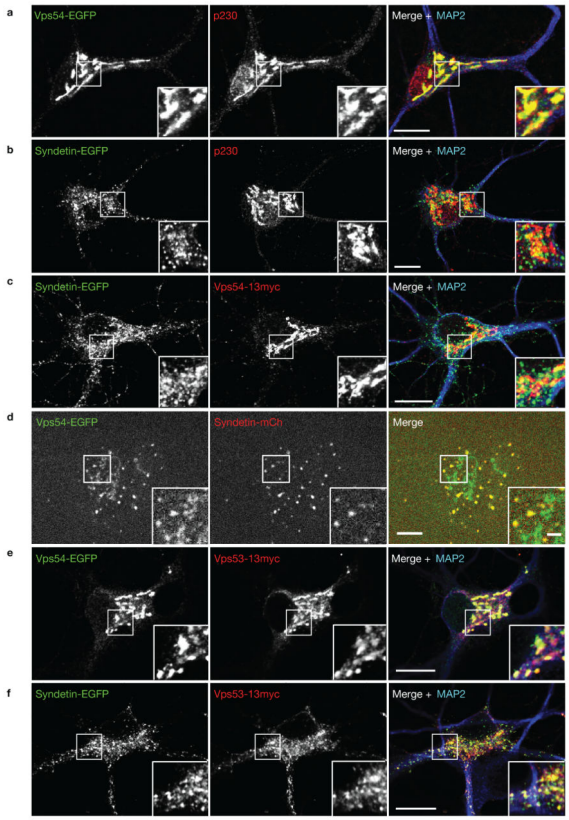

Figure 3.

Localization of Syndetin in rat hippocampal neurons and H4 cells. (**a,b**) Rat hippocampal neurons were transfected with plasmids encoding Vps54-EGFP (**a**) or Syndetin-EGFP (**b**) on day in vitro 3 (DIV-3) and processed for confocal microscopy on DIV-7. Cells were fixed and localization was determined by immunostaining with mouse antibody to GFP, rabbit antibody to p230 (TGN marker) and chicken antibody to MAP2 (somatodendritic marker) followed by Alexa488 donkey anti-mouse, Alexa555 donkey anti-rabbit and Alexa647 goat anti-chicken antibodies. (**c**) Rat hippocampal neurons were transfected with plasmids encoding Syndetin-EGFP and Vps54-13myc and immunostained with rabbit antibody to GFP, mouse antibody to the myc epitope and chicken antibody to MAP2, followed by Alexa488 donkey anti-rabbit, Alexa555 donkey anti-mouse and Alexa647 goat anti-chicken antibodies. (**d**) H4 cells stably expressing Vps54-EGFP were transfected with a plasmid encoding Syndetin-mCherry and imaged 48 h later by live-cell confocal microscopy. Images show the first frame from Movie 1. (**e,f**) Rat hippocampal neurons were transfected with plasmids encoding Vps54-EGFP and Vps53-13myc (**e**) or Syndetin-EGFP and Vps53-13myc (**f**) and processed as described in **a**,**b**. In **a-c** and **e**,**f**, bars, 10 μm; insets show 2x magnifications of the boxed areas. In **d**, bar, 6 μm; inset bar, 1.5 μm.

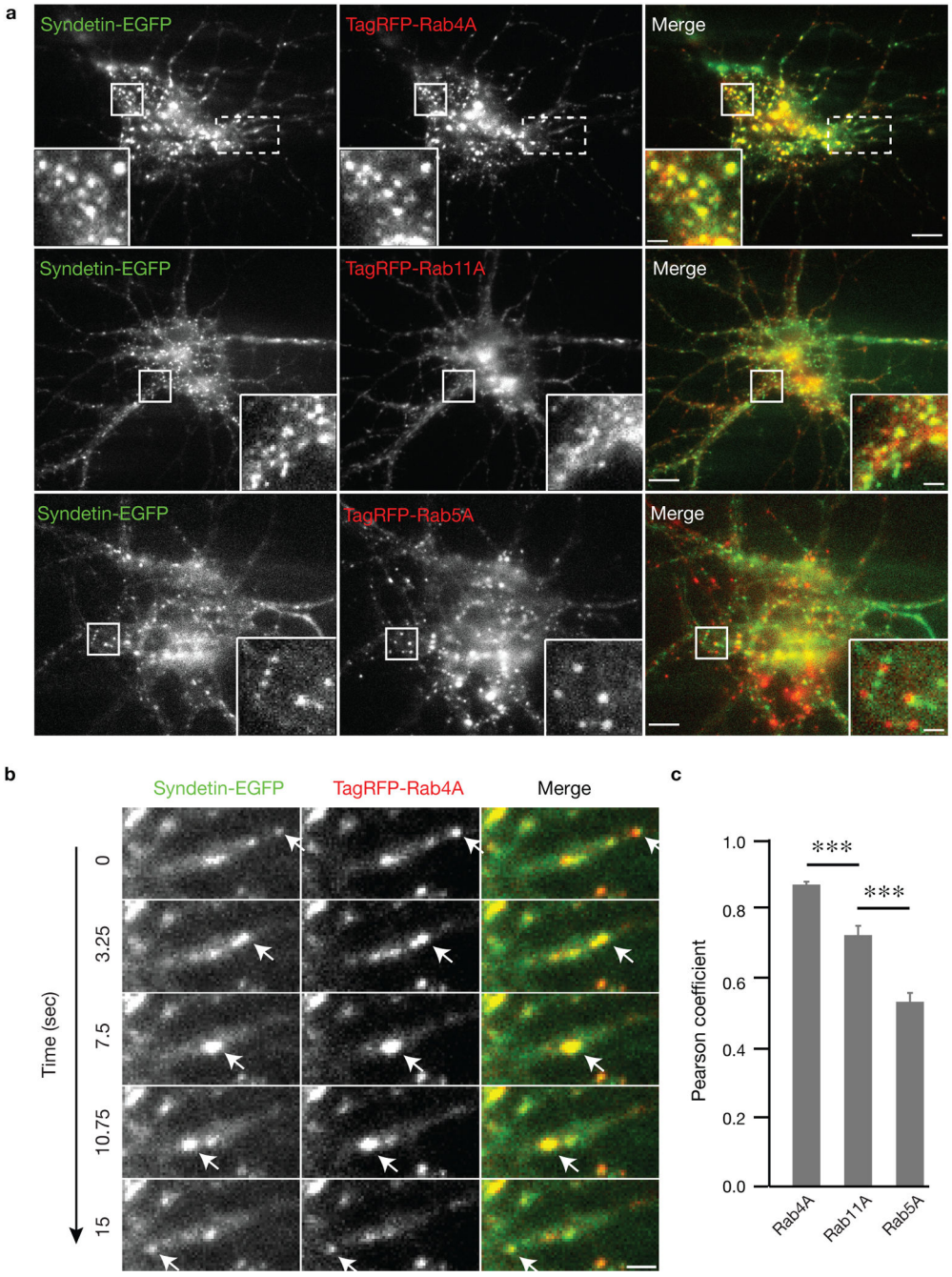

Figure 4.

Analysis of the co-localization of Syndetin with endosomal Rabs. (**a**) Rat hippocampal neurons were co-transfected with plasmids encoding Syndetin-EGFP plus TagRFP-Rab4A (upper row), TagRFP-Rab11A (middle row) or TagRFP-Rab5A (lower row) on DIV-3 and examined by TIRF microscopy on DIV-7. Shown is the first frame from live-cell imaging movies. Bars, 5 μm. Insets show magnifications of the areas boxed with solid lines. Bar, 1 μm. (**b**) Selected frames from the area boxed with dashed lines in **a** (upper row) taken from Movie 2 show a moving structure containing Syndetin-EGFP and TagRFP-Rab4A (arrows).

Bar, 2.5 μm (**c**) Quantification of Syndetin co-localization with endosomal Rabs. Pearson's correlation coefficients for Syndetin-EGFP and TagRFP-Rab4A, TagRFP-Rab5A, and TagRFP-Rab11A were calculated using ImageJ Plugin JACoP. For each group, image pairs from n=9 cells pooled from 3 independent experiments were used in the calculations. Values are the mean ± SEM. ***, $P < 0.0002$ (Rab4A vs. Rab11A) and $P < 0.0011$ (Rab11A vs. Rab5A).

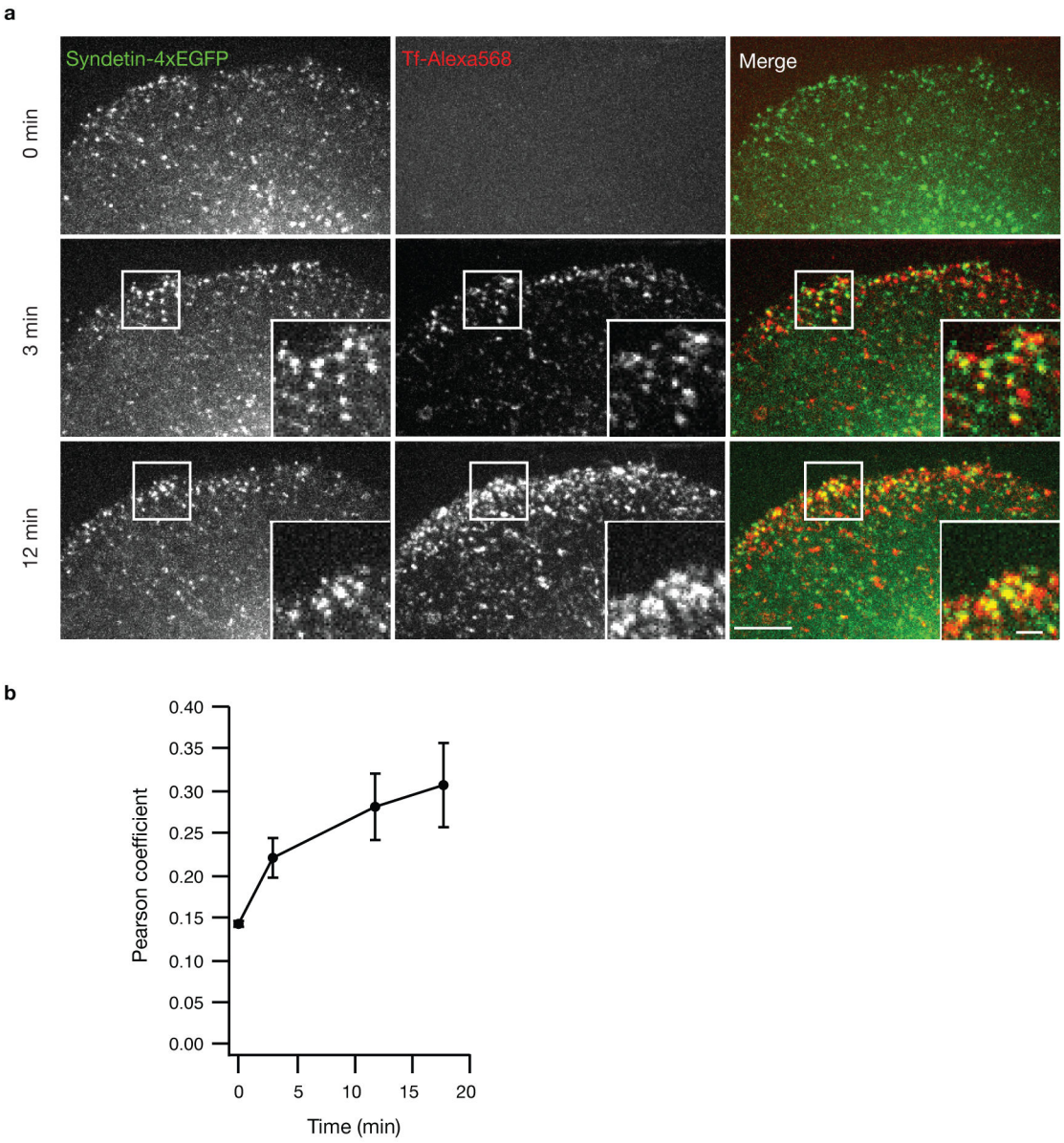

Figure 5.

Localization of internalized Tf to Syndetin-positive compartments. (**a**) HeLa cells depleted of endogenous Syndetin by siRNA treatment were transiently transfected with a plasmid encoding Syndetin-4xEGFP and imaged at 37°C in the presence of Tf-Alexa568 in the incubation medium. Images of Syndetin-4xEGFP and Tf-Alexa568 acquired at 0 (upper panel), 3 (middle panel) and 12 min (lower panel) are displayed. Bar, 5 μm; inset bar, 2 μm. (**b**) Quantification of the experiment described in **a**. Pearson's correlation coefficients for Syndetin-4xEGFP and Tf-Alexa568 were calculated using ImageJ Plugin JACoP. Image pairs from *n*=9 cells pooled from 3 independent experiments were used in the calculations. Values are the mean ± SEM.

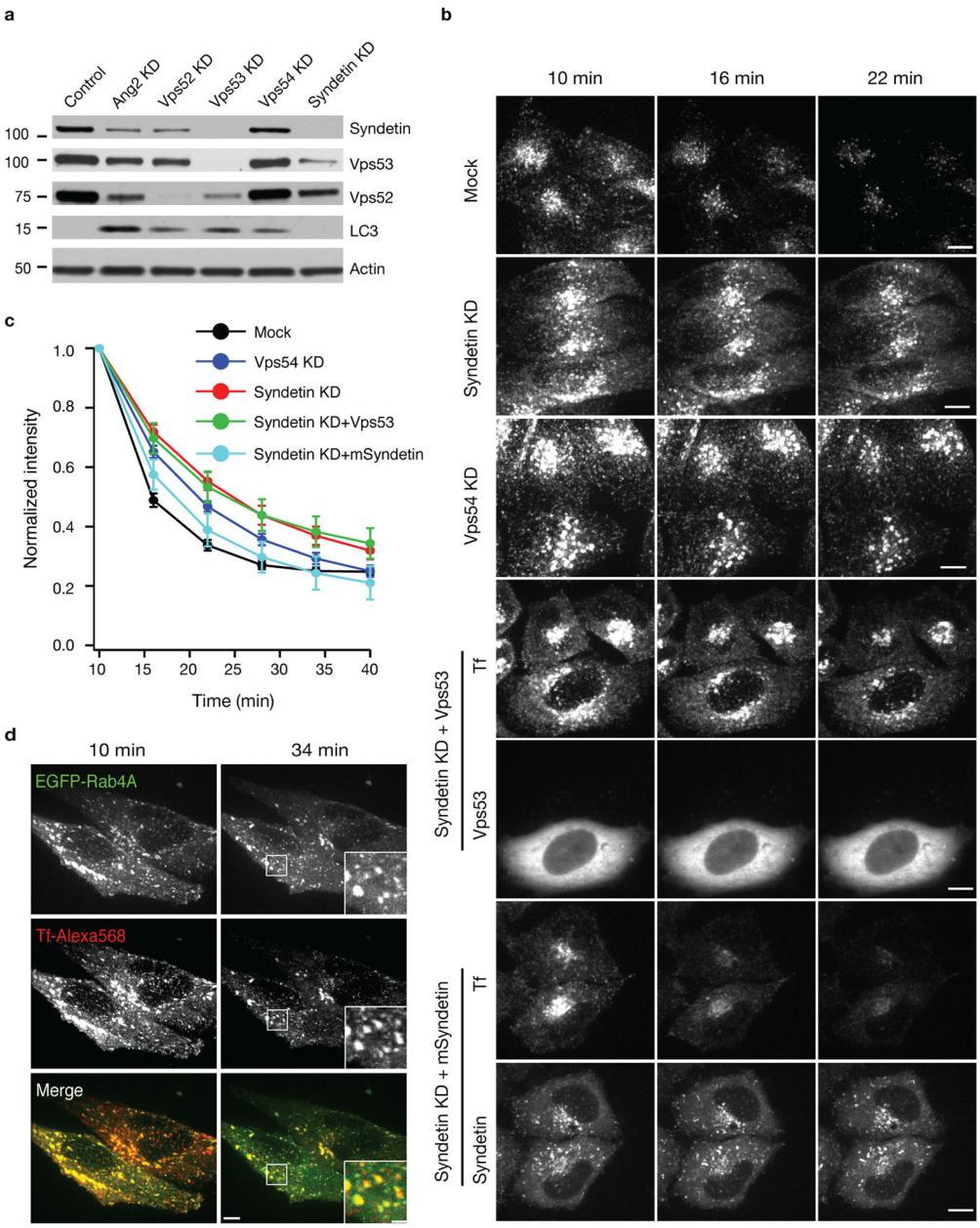

Figure 6.

Syndetin KD delays Tf recycling. (**a**) HeLa cells were treated with siRNAs targeting the proteins indicated on top and analyzed by SDS-PAGE immunoblotting for the proteins indicated at right. Molecular mass markers (in kDa) are indicated at left. Uncropped images of the blots are shown in Supplementary Fig. 5b. (**b**) HeLa cells transfected with the indicated siRNAs and plasmids encoding human Vps53 or mouse Syndetin (mSyndetin) were allowed to internalize Tf-Alexa568 for 20 min and then chased for different times at 37°C. Tf-Alexa568 fluorescence was monitored by live-cell confocal imaging. Representative maximum projection images acquired at the indicated time points are shown. Bars, 6 μm. (**c**) Quantification of Tf-Alexa568 fluorescence intensity over time. Values are

the mean ± SEM (*n*=3 independent experiments. The numbers of cells quantified were: mock, 301; Vps54 KD, 297; Syndetin KD, 250; Syndetin KD plus Vps53, 73; Syndetin KD plus mSyndetin, 61. (**d**) HeLa cells were treated with siRNA to Syndetin and transfected with a plasmid encoding EGFP-Rab4A. At 72 h after transfection, cells were allowed to internalize Tf-Alexa568 for 20 min and imaged by live-cell confocal microscopy in chase medium at the indicated time points. Bars, 6 μm; inset bar, 1.5 μm.

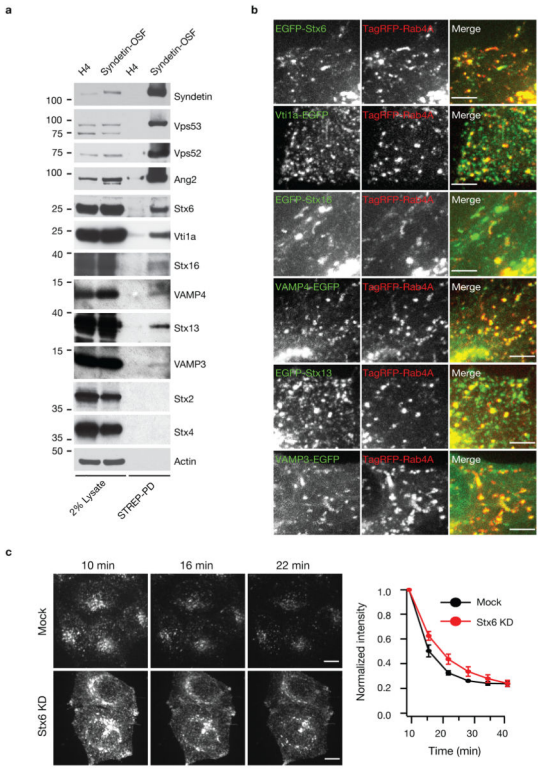

Figure 7.

EARP functions in association with Stx6 and cognate SNAREs. (**a**) H4 cells, untransfected or stably transfected with Syndetin-OSF, were cross-linked with dithio-bis-succinimidylpropionate (DSP) and lysed. Syndetin-OSF and associated proteins were pulled down on StrepTactin beads (STREP-PD) and analyzed by SDS-PAGE and immunoblotting with antibodies to the indicated proteins. Molecular mass markers (in kDa) are indicated at left. Uncropped images of the blots are shown in Supplementary Fig. 5c. (**b**) Endosomal localization of Stx6 and cognate SNAREs. HeLa cells were co-transfected with TagRFP-Rab4A and different EGFP-tagged SNAREs as indicated, and examined 24 h after transfection. Bars, 6 μm. (**c**) Mock-treated or Stx6 siRNAs-treated HeLa cells were allowed to internalize Tf-Alexa568 for 20 min and then chased at 37°C. Representative maximum projection images acquired at the indicated time points are shown. Values are the mean ± SEM (*n*=3 independent experiments. The numbers of cells quantified were: mock, 162; Stx6 KD, 143. Bars, 6 μm.

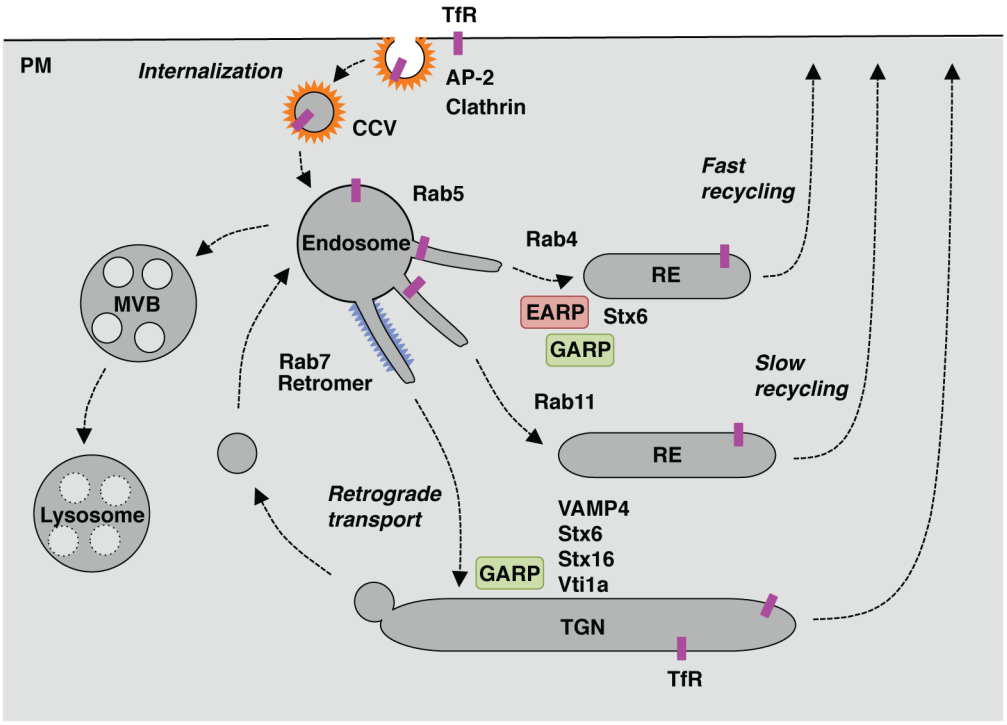

Figure 8.

Schematic representation of TfR recycling, and the roles of EARP and GARP. GARP participates in retrograde transport by promoting the assembly of the Stx6-Stx16-Vti1a-VAMP4 SNARE complex at the TGN[41], while EARP and, to a lesser extent, GARP, promote transport through recycling endosomes by acting on Stx6 in conjunction with endosomal SNAREs.